Turk J Phys
28 (2004) , 257 – 264.

Structure and Dielectric Behaviour of Barium Cupro Molybdate Ceramic

N. G. DURGE[1], M. S. NADKARNI[1] and S. V. SALVI[2]
[1] *Physics Department, S. S. and L.S. Patkar College, Goregaon, Mumbai 400 062, INDIA*
[2] *Physics Department, Institute of Science, M. C. Road, Mumbai 400 032, INDIA*

Received 10.07.2003

Abstract

The ceramic of new perovskite Ba ($Cu_{1/2}$ Mo $_{1/2}$) O_3has been synthesized at 1200 °C for 24 hours. The XRD analysis indicates an ordered hexagonal structure, which is attributed to large valency difference between octahedral cations. The IR spectrum reveals the presence of Cu-O-Mo ordered bond. The room temperature relaxation spectra imply a large conductivity term and multiple 'Debye terms' at low frequencies. This is attributed to presence of the space charge. The variation of dielectric constant with temperature has been investigated from room temperature to 800 K. The diffusivity constant equal to 1 implies normal ferroelectric behaviour near room temperature. Near 650 K, the diffusivity constant is 2 implying diffuse phase transition at 650 K. The D.C. resistivity has been measured from room to 600 °C. The PTC of resistance of the ceramic at room temperature implies ferroelectric behaviour near room temperature. The band gap is around 1.42 eV and the corresponding Schottky barrier is determined from the I-V characteristic is less than 1 Volt. In conclusion, the ceramic is a diffuse phase material having possibly the presence of ferroelectric microdomains.

1. Introduction

A(BB′) O_3 perovskites are known for relaxor behaviour [1-3]. Perovskites in which A-site is occupied by rare earth (Ba, Sr, or Ca) and octahedral site is occupied by Fe, Co, Ni, etc. are well investigated for their electrical and dielectric properties [4-6]. However, very few molybdenum containing perovskites have been synthesized for their electrical properties [7]. This has prompted us to synthesize and investigate structural and electrical properties of Ba ($Cu_{1/2}$ Mo $_{1/2}$) O_3 (BCM).

2. Experimental

Fine powders of AR grade $BaCO_3$, CuO and MoO_3 are taken in 2:1:1 molecular weight proportion. The mixture is homogenized and presintered at temperature below the melting point of MoO_3. Further, the heating is done progressively at 950 °C, 1100 °C and 1200 °C for 24 hours in each case. The sample synthesized at 1200 °C is analyzed chemically [8] particularly to determine loss of molybdenum, if any. The presence of molybdenum is 18.1 wt percent of sample, indicating no loss of molybdenum. The structural information is obtained at all the three temperatures by using powder X-ray diffraction (XRD) technique on a JEOL-JDX-8030 diffractometer (Germany). The corresponding IR absorption spectra are taken on 'PERKIN-ELMER1600' series FTIR spectrometer at room temperature from 400 cm^{-1} to 1000 cm^{-1}.

The dielectric constants and loss of these samples are measured at 1 KHz by two-probe method using an LCR meter. These measurements are carried out from room temperature to 800 K. also the the relaxation spectra are taken on 4284A precision LCR meter (HEWLETT PACKARD) from 20 Hz to 1 MHz at room temperature. The DC resistivity is measured by two-probe method from room temperature to 800 K. Finally, the I-V characteristic of ceramic is measured at room temperature.

3. Results and Discussion

All XRD patterns are indexed in hexagonal phase symmetry. Therefore, the XRD pattern and data of only sample annealed at 1200C are reported in Table 1 as typical case. However, the lattice parameters of all three samples are compared in Table 2. It is interesting to note that as the annealing temperature increases, a(Å) decreases and c (Å) increases indicating greater crystalline order at higher annealing temperature. Also, particle size increases with annealing temperature. The non zero slope of $\beta \cos\theta$ vs $\sin\theta$ indicates inhomogeneous (i.e. strained) growth of unit cell, where β is full width at half maximum of the reflection [9]. The corresponding plot for the material sintered at (1200 °C) is shown in Figure 1 as a typical case. The slope is the measure of inhomogeneous growth (Table 2) for this material. The non-zero slope means a strained growth even at 1200 °C.

Table 1. Comparison of observed and calculated d-values (Å) of reflections of BCM at room temperature.

d_{obs} (Å)	d_{cal} (Å)	I / I_0	hkl
3.341	3.340	100	312
3.197	3.168	46	301
2.771	2.775	39	221
2.098	2.097	38	225
1.875	1.873	31	414
1.697	1.695	32	334
1.389	1.390	20	531
1.356	1.355	20	620

Table 2. Structural properties of BCM at different annealing temperatures.

Sintering Temp. (°C)	Lattice constants a(Å)	c(Å)	Particle size (Å)	Inhomogeneity
950	11.438	15.341	324	0.080
1000	11.368	15.380	376	0.322
1100	11.327	15.620	409	0.070
1200	11.280	15.680	486	0.390

The IR absorption spectrum of the sample (1200 °C) is depicted in Figure 2 and the corresponding band frequencies are given in Table 3. The band around 500 cm^{-1} is observed to be broaden by well separated fine structure which is due to the increased asymmetry [11]. The band frequencies of the sample sintered at 1100 °C are also included in the Table 3 to facilitate comparison. All these bands correspond to the octahedral stretching or bending modes of the perovskite. The assignment of modes [12] and bonds [13] to different band frequencies are shown in Table 3. The very intense band corresponding to the Cu-O-Mo bands implies the order in accordance with large unit cell parameters. This band shifts to high-energy side when the annealing temperature is increased Table 3. This is consistent with corresponding decrease in the unit cell volume Table 2.

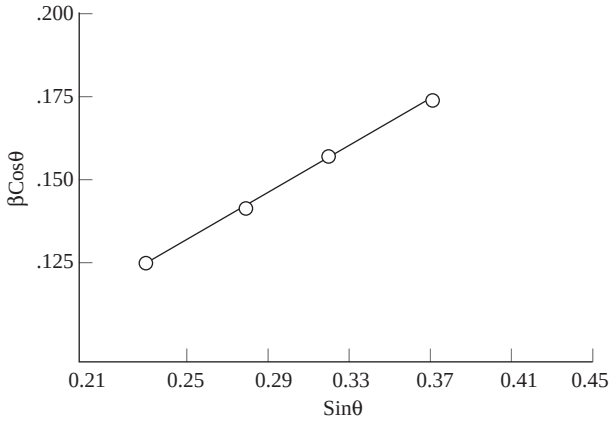

Figure 1. The $\beta \cos\theta$ versus $\sin\theta$ for BCM.

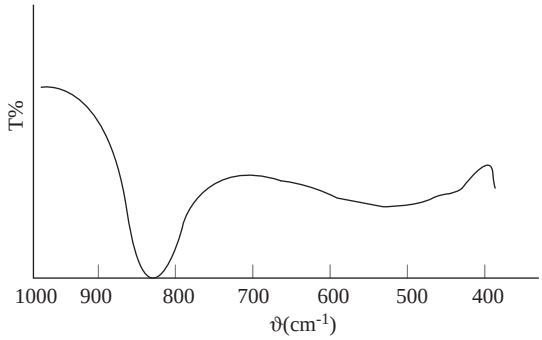

Figure 2. Infrared spectra of BCM measured at room temperature.

Table 3. IR absorption frequencies and mode of assignment of bonds in BCM.

Annealing Temperature (°C)	Infrared Frequencies (cm $^{-1}$)	Mode of assignment
1100	790 (s) ν_1	Cu – O – Mo (str)
	520 (s) ν_2	Mo – O – Mo (str)
1200	823 (s) ν_1	Cu – O - Mo (str)
	509.7 (w) ν_2	Mo – O – Mo (str)
	441.7 ν_3	Cu – O – Ni (ben)

s – strong, br – broad, M – medium, W – weak, str – stretching mode, ben – bending mode.

Figure 3 shows the frequency dependence of dielectric constant (k') and loss (k'') between 20 Hz to 1 MHz at room temperature for BCM (1200 °C). The features of the plot corresponding to k' are compared with a curve obtained for condenser model of the parallel plates designed for the interfacial polarization [14-16], where a rapid fall with frequencies in the mid frequency region, a long tail in the high frequency region are comparable. The flat low frequency region is non-existent. This may be indicative of a transition near the room temperature. The curve corresponding to the k'' is dominated by a conducting term and broad weak- relaxation frequencies at 50 Hz, 370 Hz and 1 KHz could be detected. The low value of relaxation frequencies is indicative of the formation of polar microdomains [17].

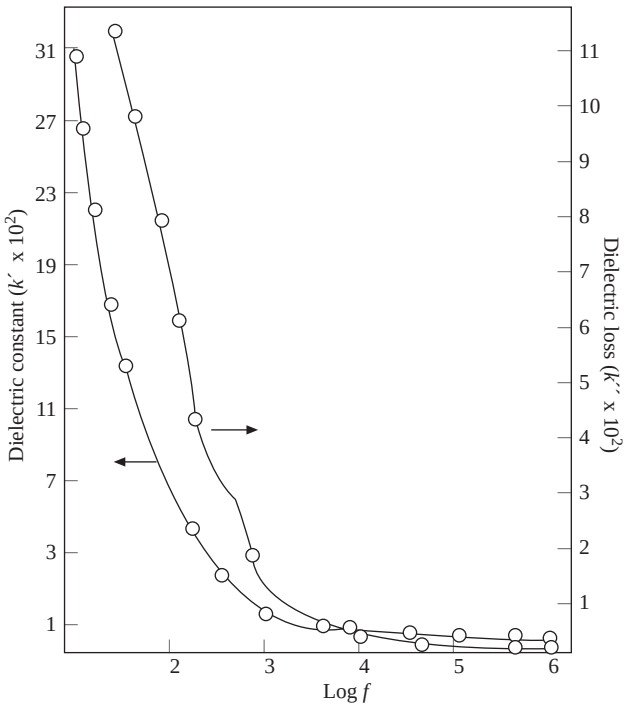

Figure 3. Dielectric constant k' and loss k'' versus logarithm of frequency for BCM.

The room temperature dielectric constants of the samples annealed at 1100 °C and at 1200 °C are compared at two different frequencies Table 4. At a given frequency, the dielectric constant is observed to increase when annealing temperature increases. Similarly, for a given sample, the dielectric constant decreases with a frequency. These trends are similar to relaxor behaviour [1,6].

Table 4. Dielectric constant at room temperature.

Sintering temperature	Dielectric constant (k') at	
(°C)	400 Hz	at 1 KHz
1100	1097	240
1200	1808	260

The dielectric constant and the loss of the ceramic annealed at 1200 °C are measured at 1 KHz from room temperature to 800 K. The curves are depicted in Figure 4. They indicate there may exist a transition below room temperature [18]. Also, there is broad transition around 650 K.

Figure 5 shows the plot of ln $(1/k' - 1/k'_{max})$ versus ln$(T - T_{max})$ for corresponding to the post transition region. The slope of graph indicates the diffuseness or diffusivity of phase transition [19]. The diffusivity (γ) = 1 corresponds to the normal Curie- Weiss type dielectric and $\gamma > 2$ implies typical diffuse transition type relaxor [19,25-27].in the present case, $\gamma = 2$, diffuse phase transition (DPT) due to the polar microdomains in the ceramic.

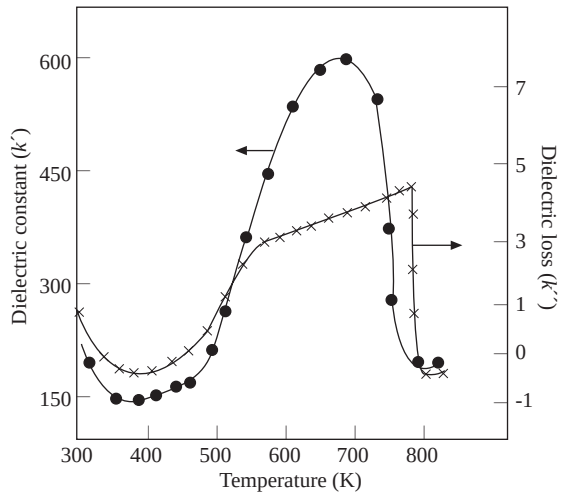

Figure 4. Dielectric constant k' and loss k'' at 1 kHz versus temperature for BCM.

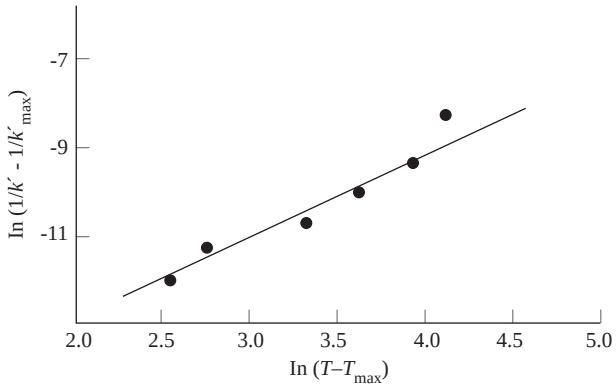

Figure 5. Variation in $\ln(1/k' - 1/k'_{\max})$ of BCM as a function of $\ln(T - T_{\max}$ at $f = 1$ kHZ.

The DPT has been explained on the several factors [19-25]. However in the present case DPT may be explained in the following manner: The smaller ionic radius of Mo $^{6+}$and large difference between valancies of Mo $^{6+}$ and Cu^{2+} is suitable for lowering the symmetry. Indeed, it causes hexagonal ordering in these perovskites. However, the lower symmetry weakens the interactions among octohedrals of different cations. This is evident from small overall values of dielectric constants of these perovskite. Therefore, the polar domains caused by the ordering may be very very small in size and non-homogeneously distributed in the material. This is responsible for DPT in this perovskite. Though the loss factor behaves as the same manner as the dielectric constant with respect to temperature, discontinuities are rather more prominent.

The room temperature resistivity of the sample (1100 °C) is 4.42 x 10^5 (Ω-cm). On the other hand sample (1200 °C) has resistivity 2.68 x 10^5 (Ω-cm). This means that the conductivity of latter sample increases by nearly 60%. The corresponding increase in the dielectric constant is also 60%. The nature of resistivity curve (ln p versus 1/T) Figure 6 of the sample 1200 °C is similar to that of the loss factor Figure 4, showing that dielectric constant and the conductivity are strongly correlated. This means that the same space charge is responsible for both dielectric constant and conductivity.

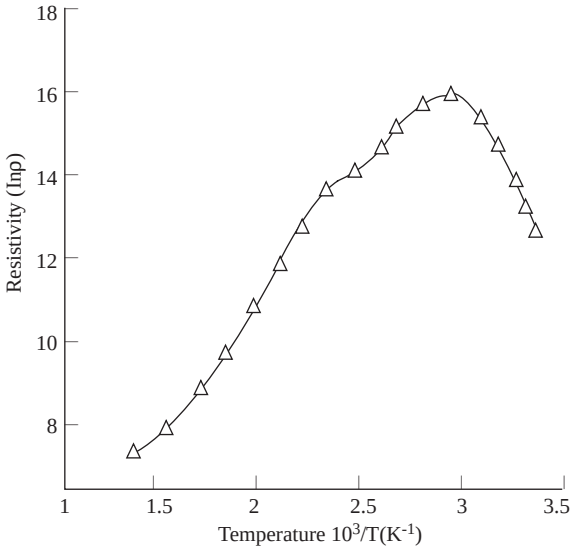

Figure 6. $\ln \rho$ versus $10^3/T$ for BCM.

Also, the plot Figure 6 indicates Positive Temperature Coefficient of Resistance (PTCR) effect just above room temperature. The PTCR effect in ferroelectric material is attributed to the ferroelectric transition [28]. Such a PTCR behaviour is explained on the basis of Heywang [29] model. The model may be applicable in the present case in the following manner.

The tendency of Mo^{6+} ion to lower the symmetry is quite obvious from the compounds of molybdenum [10] and the present hexagonal perovskite. Further, the large size of $Ba2^{+}$ ion in the barium containing perovskite is known is to cause vacancies inside the grain [30]. The number of vacancies would only be enhanced by the presence of smaller Mo $^{6+}$ ion. The barium vacancies would have effectively the negative charge carriers inside the grains. However on the grain boundaries the oxygen deficiency would effectively act as positive charge carriers. Thus, negative charge carriers are inside the grain and positive charge carriers are on the grain boundaries. Under the influence of polar microdomains due to the ordering of octahedral cations, these charges are responsible for PTCR effect in BCM.

At higher temperatures, the curves correspond to the resistivity and loss factor show a discontinuity at the same temperature. Hence, it is concluded that the losses are mainly due to the conductivity. At higher temperature, the curve indicates the semiconductor nature of the ceramic. The low temperature (362 K to 694 K) activation energy is 0.4 eV. It increases to 0.71 eV in the high temperature region. The activation energy corresponding to high temperature is taken as half the band gap. Therefore, the band gap in this material is 1.42 eV.

The I-V characteristic of BCM (Figure 7) ceramic shows a Schotkky potential barrier which is less than 1 eV, which is comparable with that obtained for $BaTiO_3$ ceramic [31].

4. Conclusion

It is concluded that the complex compound BCM (1200 °C) is a diffuse phase material with a presence of polar microdomains. A higher annealing temperature and large annealing time is likely to improve this behaviour.

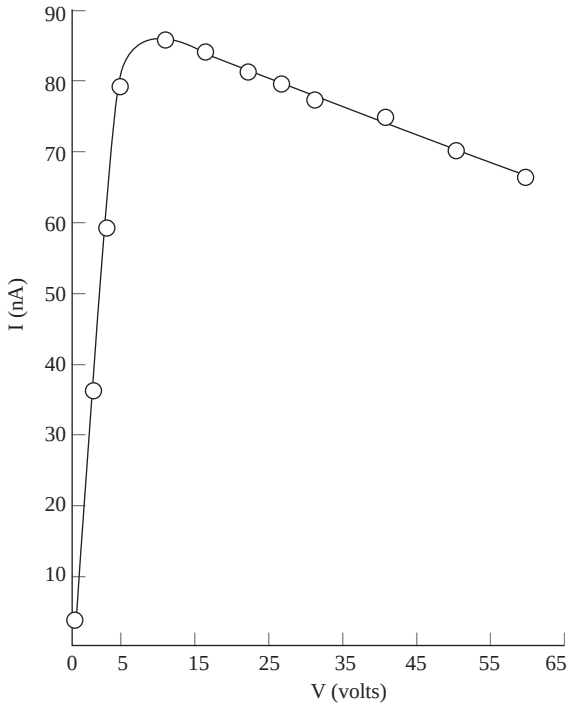

Figure 7. Room temperature I-V characteristics for BCM.

Acknowledgement

Financial support from Patkar – Varde College and Mumbai University, Mumbai, India is greatly acknowledged.

References

[1] P. Papet, T.R. Shrout and J.P. Dowhwrty, *J. Mate. Res.*, **5**, (1990), 2902.

[2] A.S. Bhalla, R. Roy and S. Komareni, *Ferroelectrics Lett.*, **11**, (1990), 137.

[3] S. Sharma, R.N.P. Choudhary, R. Sati and K.P. Sharma, *Ind. J. Pure & Applied Physics*, **31**, (1993), 200.

[4] L.H. Brixner, *J. Phys. Chem.*, **64**, (1960), 165.

[5] M.F. Kupriyanov and E.G Fesenko, *Sov. Phys.Cryst.*, **7**, (1962), 358.

[6] F.K. Patterson, K. Moller and R. Ward, *Inorg. Chem.*, **2**, (1975), 196.

[7] S.K. Mishra and D. Pandey, *J. Phys. Conden. Matter.*, **7**,(1995), 928.

[8] Kawashima, M. Nshida, I. Veda and H. Ouchi, *J. Am. Ceram. Soc.*, **66**, (6), (1983), 421.

[9] P.L. Hariharan, Ph. D. Thesis, I.I.T. Mumbai, (1978).

[10] E. Husson, L. Abelli, L.Abellor and A.Morell, *Meter. Res. Bull.*, **25**, (1990), 359.

[11] C. Barraclough, J. Lewis and R.S. Nyholm, *J. Chem Soc.*, **35**, (1959), 52.

[12] A.R. Van Hippel, "Dielectric and Waves" (John Wiley and sons Ins., New York, 1954).

[13] J.C. Maxwell, "Electricity and Magnetism", Vol. 1 (Clarendom Press, Oxford, 1982), p. 452.

[14] K.W. Wangner, in "Die Isolierstoffe der Elektrotechnik", edited by H. R Schering, (Springer Berlin, 1924), pp 1 ff.

[15] J. Kuwata, K. Uchino and S. Nomura, *Jpn. J. Appl. Phys.*, **21**, (1982), 1298.

[16] H.D. Magaw, "Ferroelectricity in crystals" (Methun, London, 1957).

[17] V.S. Dhananjai, D. Pandey and V.S. Tiwari, *J. Am. Ceramic Soc.*, **77**, (7), (1994), 1819.

[18] V.W. Kanzing, *Phys. Acta.*, **24**, (1951), 175.

[19] H.T. Martiorena and J.C. Burtoot, *J. Phys. C.*, **7**, (1974), 3182

[20] F.W. Cooke, R.C. Bradt, R.C. De Vries and G.S. Ansell *Am. Ceram. Soc.*, **49,** (1966), 648

[21] S.W. Choi, T.R. Shrout, S.J. Jang and A.S. Bhalla *Ferroelectrics*, **100**, (1966), 29.

[22] Kuwata, K. Uchino and S. Nomura, *Jpn. J. Appl. Phys.*, **21**, (1982), 1298.

[23] G.A. Smolensokii, *J. Phys. Soc. Jpn.*, **28**, (1970), 26.

[24] P. Groves, *J. Phys. C.*, **19**, (1986), 111.

[25] H. Neumann, G. Arlt *Ferroelectrics*, **69**, (1986), 179.

[26] J.G. Fogan and Vasantha and R.W. Amarakoon, *J. Am. Ceram. Soc.*, **72**, (2), (1993), 69.

[27] I.P. Raevskii, *Sov. Phys. Solid state*, **28**, (10), (1983), 1375.

[28] W. Heywang, *Solid State Electron*, **3**, (1), (1961), 57.

[29] A.F. Well, "Structural inorganic chemistry" 5^{th}, Ed. pp. 558.

[30] F.K. Patterson, C.W. Moller and R. Warel, *Inorganic Chem.*, **2**, (1975), 196.

[31] G. Blarse, *Inorg. Nucl. Chem.*, **34**, (1972), 3401.

[32] V.M. Gwzevich, Electric Conductivity of ferroelectric, Israel Program for Scientific Translation Ltd. IPST cat. No. 5915, (1971).

[33] K. Sambasiva Rao, *Ind. J. of Pure and Appl. Phys.*, **21**, (1993), 43.